Crystal-field effects on the thermal conductivity of localized spin metallic compounds

A. Rassili*
Institute of Physics B5, University of Liège, Sart-Tilman, B-4000 Liège, Belgium

K. Durczewski†
Institute for Low Temperatures and Structure Research, Polish Academy of Sciences, P.O. Box 1410, PL-50 950 Wroclaw 2, Poland

M. Ausloos‡
Institute of Physics B5, University of Liège, Sart-Tilman, B-4000 Liège, Belgium

(Received 2 December 1997; revised manuscript received 20 April 1998)

The influence of the crystal-electric-field (CEF) splitting on the thermal conductivity is calculated on the basis of a two-level system model applicable to intermetallic magnetic compounds. The localized spin scattering contribution κ_s, in a manner similar to the total electronic thermal conductivity κ_e, shows a larger increase at low and intermediate temperatures as compared to the case in which no crystal-electric-field splitting is taken into account. The influence of some theoretical parameters is also discussed. It is shown that the CEF effect enhances the effect of the magnetic scattering potential, and impurity contributions screen such an enhancement at temperatures below the Debye temperature. Other scattering contributions, e.g., electron-phonon and electron impurities, are also taken into account in our calculation. The theory is in quantitative agreement with data on $R\mathrm{Al}_2$ systems taken as test cases, and leads to values of the level splitting in the 50 K range. [S0163-1829(98)03133-6]

I. INTRODUCTION

The influence of the $4f$ levels of the rare-earth ions on the transport properties of localized spin metallic compounds is called either specific[1] or strong.[2] Theoretical models investigating this influence have been presented in a limited number of publications only.[3–5] The case of thermal conductivity does not seem to have been worked out.

In previous investigations[6–9] we have calculated the thermal conductivity of localized spin metallic compounds using a variational method taking into account several scattering processes, i.e., e^- phonon, e^- impurity, and e^- localized spin. Their contributions were clarified. Continuing in the same path, we show in the following the influence of the crystal-electric-field splitting on the thermal conductivity on the basis of a two-level system model. It will be found that the localized spin scattering contribution κ_s, in a manner similar to the total electronic thermal conductivity κ_e, shows an increase at low temperatures as compared to the case in which no crystal-electric-field splitting is taken into account.

The splitting of *f*-shell energy levels of rare-earth ions in a crystal by the electric field surrounding ions [crystal-electric field (CEF)] is an intrinsic property. It is known that magnetic properties of rare-earth compounds depend on whether the ground state of the shell is a singlet or a multiplet.[10] For instance, if a magnetic (indirect) exchange interaction, e.g., via the conduction electrons, exists in the singlet ground state system, a spontaneous magnetic order can exist below a finite temperature only in the case of a sufficiently strong exchange interaction. This fact was discovered by Bleaney in the 1960's,[11] and discussed, e.g., in Ref. 12.

The magnetic order ground state will not be the main subject of the following investigation, but we shall study the results on the thermal conductivity due to conduction electron scattering by a doublet due to a crystal-electric field. For simplicity we consider only a shell model with $J=\frac{1}{2}$, i.e., the so-called pseudospin model and will try to examine whether the energy gained or lost by an electron in such a scattering process can be seen on a transport property. This seems more appropriate in order to gain some first insight. We shall use the known transverse Ising model picture, which together with the molecular field approximation that we apply, is a paradigm for most systems as, e.g., discussed in Refs. 11 and 12.

In Sec. II the two-level Hamiltonian expression is briefly recalled. In Sec. III we calculate the conduction-electron-localized spin scattering cross section in such a CEF case. The effect of the latter on the thermal conductivity and some discussion are found in Sec. IV. A quantitatively successful comparison to data on cubic $R\mathrm{Al}_2$ shows the interest of such investigations.

II. MODEL

Treating a complete crystal-electric-field Hamiltonian is very difficult. One should notice that each spin level is split differently by a magnetic field and usually has to consider whether the ground state is a singlet or not.[11] From there, simplifications can be made.

The interaction Hamiltonian describing the energy of localized moments can be assumed to have the form of the pseudospin ($J=\frac{1}{2}$) transverse Ising model where the transverse magnetic field Δ describes an internal electric-field effect. The Hamiltonian reads

$$H^s=\Delta\sum_i J_i^x-\sum_{i,j} K(R_i-R_j)J_i^zJ_j^z, \qquad (2.1)$$

where Δ is the strength of the crystal-electric field, J_i^μ is the μ component of the total (localized) angular momentum, and R_i denotes the lattice site coordinates. The first sum describes the crystalline-electric-field effect and the second one a ferromagnetic coupling of Ising type $[K_{xx}=K_{yy}=0,\ K_{zz}=K(R_i-R_j)]$. A more exact form of the CEF Hamiltonian, for example, in lave phases such as $R\mathrm{Al}_2$, is described in Ref. 10. Note that the Hamiltonian (2.1) describes the Bleaney model[11,12] which as a first approximation considers that only the lowest level splitting is relevant for the main scattering processes, magnetic ground state nature, and magnetic transitions. In the molecular field approximation (MFA) (Ref. 12) Eq. (2.1) can be written as follows:

$$H^s=\Delta\sum_i J_i^x-\mathcal{N}K(0)\sigma\sum_j J_j^z=\sum_i H^{(i)}. \tag{2.2}$$

After some algebra within MFA (see the Appendix) the following equation for $\sigma=\langle J_i^z\rangle$ is obtained:

$$\sigma=\frac{1}{2}\frac{A^2-1}{A^2+1}\tanh(\sqrt{\Delta^2+h_z^2}/2k_BT), \tag{2.3}$$

where

$$h_z=K(0)\sigma. \tag{2.4}$$

In the limit $T\to 0$ this equations yields the solution

$$\sigma=\frac{1}{2}\frac{A^2-1}{A^2+1}\ \text{ if }\ K(0)>2\Delta$$

and (2.5)

$$\sigma=0\ \text{ if }\ K(0)\leqslant 2\Delta.$$

For $K(0)\leqslant 2\Delta$ we have a paramagnetic system for $0<T<\infty$.

The total crystal-electric-field energy splitting Δ in simple magnetic compounds can be as large as few hundred K, e.g., 400 K for PrS, but the two lowest levels can be only distant of 50 K or so.[1] In the case of $R\mathrm{Al}_2$ compounds, the total spin level distribution can be large but the lowest level splitting is also of moderate magnitude, i.e., 30–150 K.[1,13,14] Thus, it might influence transport coefficients far below the Debye temperature ($\approx$300 K) as we are going to examine on the thermal conductivity.

III. LOCALIZED SPIN-CONDUCTION ELECTRON SCATTERING CROSS SECTION

In order to calculate the thermal conductivity, we use kinetic theory. In order to do so we should calculate cross sections and introduce them into standard formulas such as those given by linear response theory[15,16] or a relaxation time approximation.[17] For describing the scattering process we have considered the interaction between magnetic localized moments and a conduction-electron system assumed to have the form[18]

$$H_{s-f}=-(G/\mathcal{N})\sum_{l,\mathbf{k},\mathbf{k}'}\{e^{i(\mathbf{k}-\mathbf{k}')\cdot\mathbf{r}_l}(a^+_{\mathbf{k}\uparrow}a_{\mathbf{k}'\uparrow}-a^+_{\mathbf{k}\downarrow}a_{\mathbf{k}'\downarrow})J_l^z + a^+_{\mathbf{k}\uparrow}a_{\mathbf{k}'\downarrow}J_l^- + a^+_{\mathbf{k}\downarrow}a_{\mathbf{k}'\uparrow}J_l^+\}, \tag{3.1}$$

where $J_l^\mu=J^\mu(\mathbf{r}_l)(\mu=z,+,-)$ is the effective angular momentum, the Fermi operators $a^+_{\mathbf{k}v}$, $a_{\mathbf{k}'v}$ describe the electron gas, and $\mathcal{N}$ is the number of lattice sites. G is a strength constant.

The Hamiltonian (3.1) is treated as a perturbation to H^s, given in Sec. II, for static properties and an estimate of the critical temperature T_C, but Eq. (3.1) is fundamental for the scattering. Thus, in the first Born approximation the transition rate (cross section) reads

$$\mathcal{C}^s=\mathcal{C}_0\beta f(\mathbf{k})[1-f(\mathbf{k}')]\mathcal{C}(\mathbf{q},\omega), \tag{3.2}$$

where $\mathbf{k}$, $\mathbf{k}'$ $(=\mathbf{k}+\mathbf{q},)$ are, respectively, the wave vector of the conduction electron before and after the scattering for the corresponding energies $\varepsilon'(\mathbf{k}')=\varepsilon(\mathbf{k})+\omega(\mathbf{q})$, while $\mathcal{C}_0$ is a material constant[6] and

$$\mathcal{C}(\mathbf{q},\omega)=\frac{1}{\mathcal{N}}\sum_{i,j}e^{-i\mathbf{q}(\mathbf{R}_i-\mathbf{R}_j)}\int_{-\infty}^{\infty}dt e^{+i\omega t/h}\langle\mathbf{J}_i(t)\mathbf{J}_j(0)\rangle, \tag{3.3}$$

where $\langle\cdots\rangle$ means a thermodynamical average. The current time dependence is obtained through the usual Liouville equation with the Hamiltonian (3.1).

In the MFA, we calculate the long-wave range limit of Eq. (3.3) and obtain

$$\begin{aligned}\mathcal{C}(0,\omega)=&\frac{1}{2Z}\sum_{\alpha,\beta}e^{-\beta\varepsilon_\alpha}[\langle\varepsilon_\alpha|J^+|\varepsilon_\beta\rangle\langle\varepsilon_\beta|J^-|\varepsilon_\alpha\rangle\\ &+\langle\varepsilon_\alpha|J^-|\varepsilon_\beta\rangle\langle\varepsilon_\beta|J^+|\varepsilon_\alpha\rangle]\delta(\omega+\varepsilon_\alpha-\varepsilon_\beta)\\ &-\langle J^+\rangle\langle J^-\rangle\delta(\omega)+\frac{1}{Z}\sum_{\alpha,\beta}e^{-\beta\varepsilon_\alpha}[\langle\varepsilon_\alpha|J^z|\varepsilon_\beta\rangle\\ &\times\langle\varepsilon_\beta|J^z|\varepsilon_\alpha\rangle]\delta(\omega+\varepsilon_\alpha-\varepsilon_\beta)-\langle J^z\rangle^2\delta(\omega),\end{aligned} \tag{3.4}$$

where ε_α, ε_β $(\alpha,\beta=1,2)$ are the eigenvalues of $H^{(i)}$ of Eq. (2.2) $\langle\cdots|\cdots|\cdots\rangle$ denote matrix elements, and $Z=\Sigma_\alpha e^{-\beta\varepsilon_\alpha}$. $\delta(u)$ is the Dirac delta function which describes the conservation of energy in scattering processes over different energy shells.

As in a previous paper[7] we have solved the linearized Boltzmann equation by using the Ziman variational method[19,20] and by assuming a general Mathiessen rule.[6,7] We have taken into account phonon, impurity, and magnetic contributions on the same footing with the same trial functions as in Refs. 6 and 7 but with the MFA Hamiltonian (2.2) containing a crystal-field term. The latter contribution is described by matrix elements, which for the degenerated electron gas with the Fermi energy counted from the bottom of a parabolic band read

$$\mathcal{P}^s_{11}=\Pi(T), \tag{3.5}$$

$$\mathcal{P}^s_{12}=\mathcal{P}^s_{21}=\frac{2}{3}\left(\frac{\pi^2}{3}\right)\left(\frac{k_BT}{\varepsilon_F}\right)\Pi(T),$$

$$\mathcal{P}^s_{22}=\left(\frac{\pi^2}{3}\right)\Pi(T)-\Lambda(T)/2,$$

with

$$\Pi(T)=\frac{3}{4}\,(1-\overline{\sigma}^2),$$

$$\Lambda(T)=\frac{(\pi^2/3)\overline{\sigma}}{2[\cosh(x)+1]}\,x-\frac{1}{2}\,\frac{\overline{\sigma}}{\sinh(x)}\,x^2, \tag{3.6}$$

$$x=\frac{h}{k_BT}=\frac{\sqrt{\Delta^2+h_z^2}}{k_BT}, \tag{3.7}$$

and

$$\overline{\sigma}=\sigma\,\frac{A^2+1}{A^2-1}, \tag{3.8}$$

where σ and $h_z=K(0)\sigma$ should be determined from Eq. (2.5). The detailed calculations are given in the Appendix.

IV. THERMAL CONDUCTIVITY

The same assumptions as in Refs. 7–9 will be used here for pursuing the calculation. The expression of the conduction-electron-localized spin scattering contribution to the thermal conductivity (κ_s), as well as the total electronic thermal conductivity (κ_e), are given by

$$\kappa=\frac{\pi^2}{3}\,\frac{J_0^2}{P_0}\,\varepsilon_F^3(L_0T)\,\frac{1}{\mathcal{P}_{11}}\times\left[\frac{\mathcal{P}_{11}}{\mathcal{P}_{22}}-\left\{\frac{\mathcal{P}_{12}}{\mathcal{P}_{22}}-\frac{3}{2}\left(\frac{k_BT}{\varepsilon_F}\right)\left(1+\frac{\pi^2}{3}\,\frac{\mathcal{P}_{11}}{\mathcal{P}_{22}}\right)\right\}2\right], \tag{4.1}$$

where the $\mathcal{P}_{ij}$'s result from the linear representation (in a Mathiessen rule analogy) of the conduction electron-localized spin scattering $\mathcal{P}^s_{ij}$ and the other scattering mechanism matrix elements, such as $\mathcal{P}^{\rm ph}_{ij}$ for the electron-phonon scattering as calculated in Refs. 6 and 7 and $\mathcal{P}^{\rm imp}_{ij}$ for the electron-impurity scattering,[7] i.e.,

$$\mathcal{P}_{ij}=\mathcal{P}^{\rm ph}_{ij}+\varphi\mathcal{P}^{\rm imp}_{ij}+\gamma\mathcal{P}^s_{ij}, \tag{4.2}$$

where the dimensionless coefficients (γ) and (φ) measure the relative magnetic and impurity to phonon contribution in the scattering cross section, respectively.[6,7] One should notice that a mere conduction-electron-localized spin term κ_s, can be calculated using Eqs. (4.1) and (3.6). However, notice from the above that we do not calculate a mere superposition of relaxation times, i.e., we do not simply write

$$\kappa_e^{-1}=\kappa_{e\text{-ph}}^{-1}+\kappa_{e\text{-imp}}^{-1}+\kappa_{e\text{-}s}^{-1}. \tag{4.3}$$

The values of the coefficients γ and φ were estimated by us in the above quoted papers based on experimental data. They are of the order of the data presented in Table I, which we use in the present paper to illustrate our results.

The phonon contribution, treated in the same approximation as in Ref. 6, is an important background of the numerical data which we present below. As is obvious from considerations in Ref. 6 the magnitude of this contribution is determined by the parameter $2k_F/q_M$ of Table I. It denotes the ratio of the Fermi surface caliper to the phonon wave number cutoff. The values in Table I correspond to reasonable values of the Fermi energy, effective electron mass, and sound velocity.

TABLE I. Theoretical parameter values used for calculating the thermal conductivity curves illustrated in Figs. 1–6. T_F/T_D is taken to be always equal to 160 for illustration.

	$2k_F/q_M$	γ	φ
a	4	0.12	0
b	4	0.12 ($T_c=0$)	0.04
c	4	0.2	0.04
d	4	0.12	0.045
e	4	0.12	0.04
f	4	0.12	0.035
g	3.8	0.12	0.045

To compute the localized spin contribution κ_s we simply put $\mathcal{P}_{ij}=\mathcal{P}^s_{ij}$ into Eq. (4.1); since the $\mathcal{P}^s_{ij}$'s are related to the phonon background the final values of κ_s depend also on $2k_F/q_M$. The detailed formulas and calculations are found in the Appendix.

To start our discussion of the numerical results we present in Fig. 1 the results for the total electronic thermal conductivity κ_e for different physical parameters (a), (b), (d), (f). The experimental data for the $TbAl_2$ compound are also presented for a qualitative comparison and in order to observe the features of interest.

The strictly theoretical divergence of κ_e at $T=0$ is a feature to be removed by including the impurity scattering.[4,7,19] By a proper choice of the constant φ one is also able to adjust the theoretical curves to experimental data at least in the low-temperature regime.[3] The magnetic scattering manifests itself by a break at T_c,[1] here taken $T_c=0.38T_D$, where T_D denotes the Debye temperature. The slope of κ_e at intermediate and high temperature is controlled by the value of

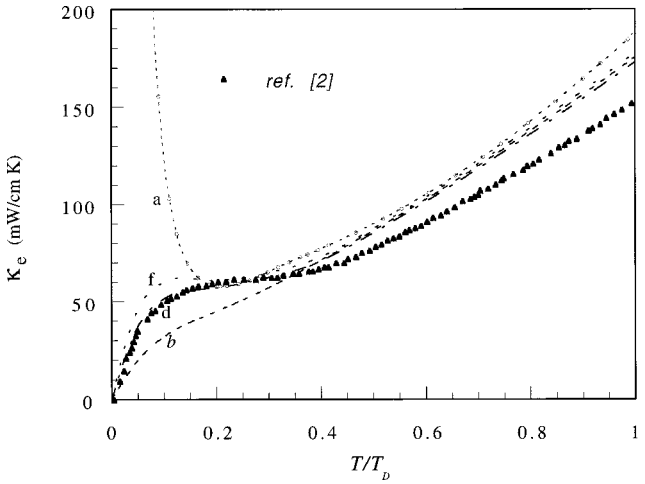

FIG. 1. Total electronic thermal conductivity κ_e as derived from Eq. (4.1) as a function of T/T_D for material data (a), (b), (d), and (f) of Table I with $\Delta=0$ circles [(a) curve] correspond to the theoretical impurity free case and the small triangles represent the experimental data of $TbAl_2$ from Ref. 2.

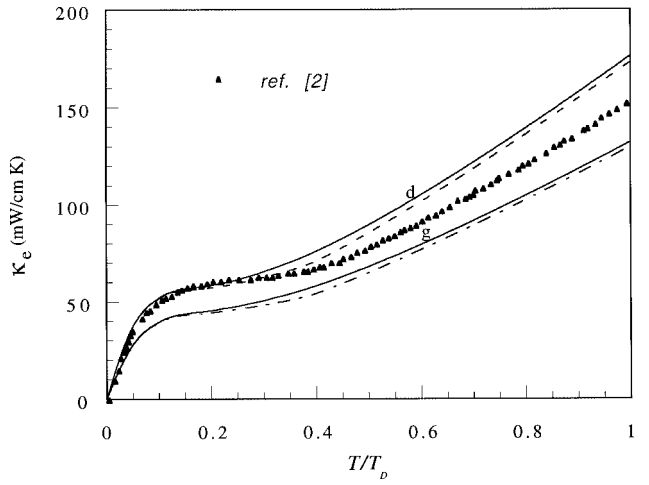

FIG. 2. Representation of the total thermal conductivity with (solid curve) or without (dash curve) CEF splitting. The influence of the cutoff wave number is shown by curves (d) and (g) and the small triangles represent the experimental data.

$2k_F/q_M$ (Fig. 2), where the results correspond to the material constants in the (d) and (g) cases of Table I for $\Delta=0$ (dash line) and $\Delta=200$ K (solid line). The same experimental data in Fig. 1 are also presented in Fig. 2.

In Fig. 3 we present the dependence of κ_S on T/T_D for the material constants (e) of Table I in the case $\Delta=0$ (dash line) and $\Delta=200$ K (solid line). For comparison we show as an inset the results for the purely paramagnetic system [item (b) of Table I] also in the case $\Delta=0$ and $\Delta=200$ K, marking the curves in the same way. It is seen that the crystal field increases the magnetic contribution to the thermal conductivity.

Figure 4 shows the localized spin contribution κ_S as a function of T/T_D. Here, by presenting the results for the items (e) and (d) of Table I we show that an increase in γ (the magnetic to phonon scattering strength) implies a decrease in the localized spin contribution κ_S.

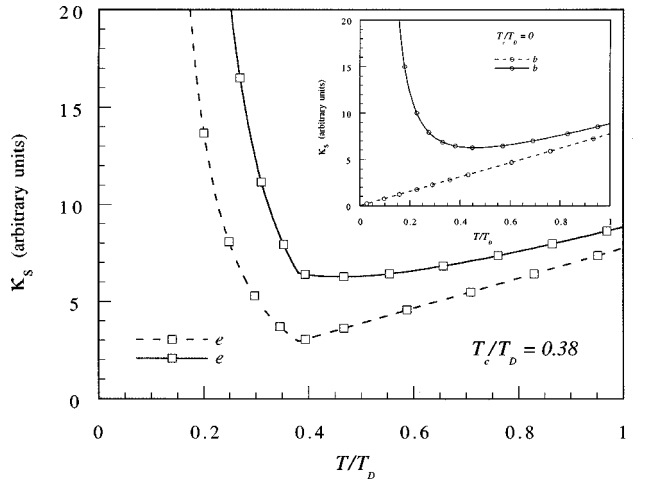

FIG. 3. Localized spin contribution to the thermal conductivity κ_S vs T/T_D computed as described in the text for the material constant (e) of Table I for $\Delta=200$ K (solid line) and $\Delta=0$ (dash line). The inset shows the dependence of κ_S for a purely paramagnetic system [item (b) of Table I].

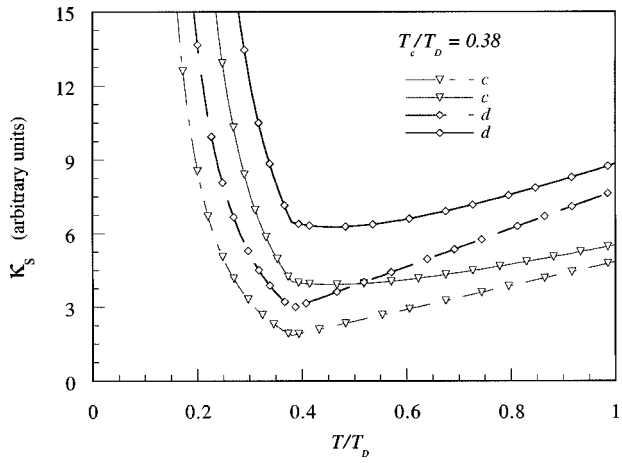

FIG. 4. Localized spin contribution κ_S to the total electronic thermal conductivity vs T/T_D for the (c) and (d) material constants of Table I in the case $\Delta=0$ (dash line) and $\Delta=200$ K (solid line).

In order to illustrate the effect of the crystal-field splitting on the total electronic thermal conductivity κ_e, we have made a plot of $\Delta\kappa=\kappa_\Delta-\kappa_0$ (κ_Δ is κ_e for $\Delta\neq0$ and κ_0 for $\Delta=0$) versus T (Fig. 5) for the material constants compiled in Table I. The value of $\Delta\kappa$ is positive in accordance with the data of Figs. 3 and 4. The only exception, i.e., when $\Delta\kappa<0$ is the case of $\varphi=0$ [item (a) of Table I], where no impurity scattering is taken into account.

It is emphasized that in cases when the system is ferromagnetic and scattering on impurities is taken into account there is a maximum of $\Delta\kappa$ in the close vicinity of the Curie temperature. In cases (a) and (b) (paramagnetic system) the maximum is shifted considerably below $T/T_D=0.38$. These two cases are marked in Table I. It is also worth to notice that the value of $\Delta\kappa$ is enhanced with an increase of γ [(c) case] as seen from Fig. 5.

The magnitude of the $\Delta\kappa$ difference in cases (c)–(g) of Table I for a given temperature is seen to be an increasing function of the crystal-field-splitting Δ, which is shown in Fig. 6 for the material constants (c). Our investigations show

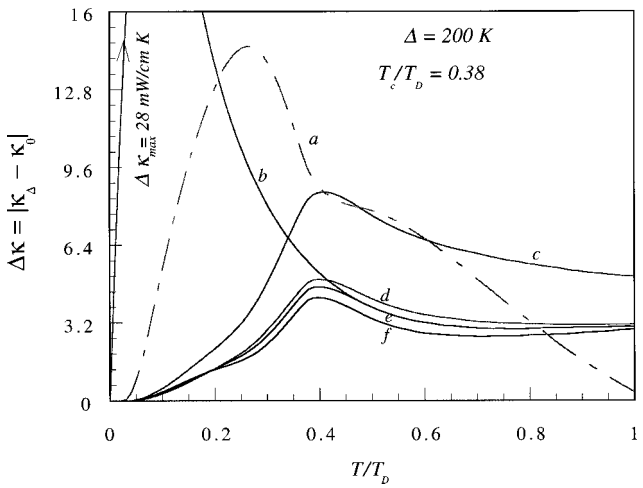

FIG. 5. The difference $\Delta\kappa$ between the electronic thermal conductivity for $\Delta=200$ K and $\Delta=0$ as a function of T/T_D. Different curves correspond to different parameter values given in Table I. In nonparticular cases the largest value of $\Delta\kappa$ is situated at T_c.

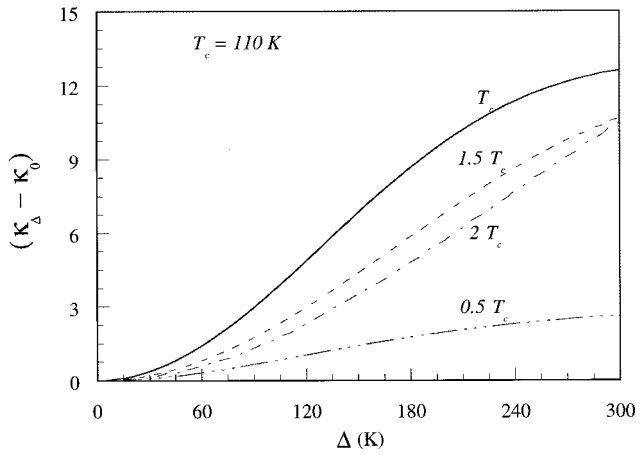

FIG. 6. The behavior of the difference $(\kappa_\Delta - \kappa_0)$ as a function of Δ for different temperatures in the case of the material constants (c) of Table I.

that this also holds true for other material constants except cases (a) and (b).

It is possible to go beyond the qualitative picture, taking into account data on a few rare-earth (R) based cubic intermetallic systems, such as RAl_2. In seven cases the thermal conductivity seems to have been measured and to fall into three categories according to the atomic number (f-shell filling or angular momentum) of the R, T_c, and Δ, in view of the overall behavior of the thermal conductivity. Examining the three different categories, we show in Fig. 7 a fit of the above formulas to one experimental datum in each category for parameter values given in Table II. The fits are rather remarkable in view of the small number of parameters and their sensitivity.

V. CONCLUSION

A simple model was used to describe the effect of the crystal-electric-field splitting on the behavior of the thermal conductivity of localized spin metallic compounds. This effect can be relevant at low, intermediate, and high temperatures. We show that there is some competitiveness between the crystal-electric field and the impurities from a scattering contribution point of view. The inclusion of the impurity scattering can change the sign of $\Delta\kappa = \kappa_\Delta - \kappa_0$ (see Fig. 5) and can considerably lower the absolute value of $\Delta\kappa$. Therefore, we can state that the presence of impurities screens the CEF splitting effect in the thermal conductivity and mainly the cases of large magnetic scattering or in a pure paramagnetic system strong influence can be found if Δ is finite.

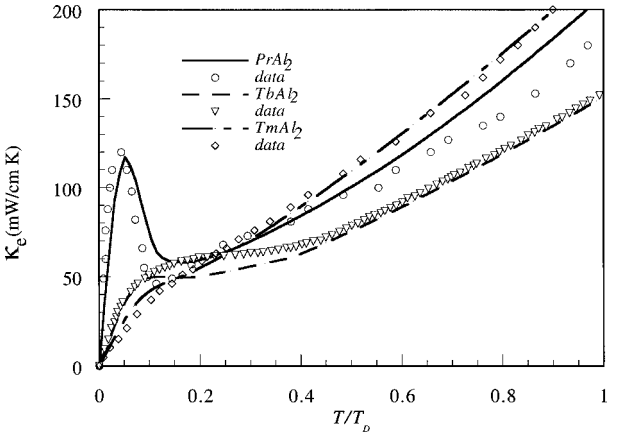

FIG. 7. Comparison of experimental data (from Ref. 2) for three distinctly different thermal conductivity behaviors. The theoretical fits use the parameters indicated in Table II.

The theory leads to quite good agreement with available experimental data on appropriate systems. Other theoretical considerations could be made in further work such as taking into account a more complicated crystal-electric-field potential[13] to investigate its effect on the behavior of transport properties of various intermetallic compounds. It seems from the above comparison with experimental data[2] that the model well describes the behavior of the thermal conductivity and that it is not necessary to generalize the model approximation, such as the MFA for the spin Hamiltonian or the simple parabolic band structure at this stage, without detailed experimental data in various temperature regimes. Moreover the simple variational method used above seems well controlled and appropriate. It is easily understood that generalized trial functions could be used in order to describe more complicated symmetries and level splittings beyond the doublet level. Nevertheless the above theory shows that a transport property such as the thermal conductivity can probe crystal-field effects in magnetic or nonmagnetic systems.

ACKNOWLEDGMENTS

This work was partially supported by ARC 94-99/174, and by a KBN (PL)-CGRI (RW) bilateral agreement.

APPENDIX

The single-site Hamiltonian $H^{(i)}$ in Eq. (2.2) is not diagonal in the representation of the eigenvalues of J^z;

$$J^z|n\rangle = (n-3/2)|n\rangle, \quad n=1,2, \tag{A1}$$

but it can be represented as

$$H=\begin{bmatrix} H_{11} & H_{12} \\ H_{21} & H_{22} \end{bmatrix} = \begin{bmatrix} h_z/2 & \Delta/2 \\ \Delta/2 & -h_z/2 \end{bmatrix}, \tag{A2}$$

where $h_z = K(0)\sigma$. The eigenvalues of H are

$$\varepsilon_1 = \frac{1}{2}\sqrt{\Delta^2+h_z^2}, \quad \varepsilon_2 = -\frac{1}{2}\sqrt{\Delta^2+h_z^2}. \tag{A3}$$

Let us define for later use the eigenvalue splitting

$$h = \varepsilon_1 - \varepsilon_2 . \tag{A4}$$

The eigenvectors $|\varepsilon_\alpha\rangle$ $(\alpha=1,2)$ are

$$|\varepsilon_\alpha\rangle = \sum_{n=1}^{2} w_{n\alpha}|n\rangle \tag{A5}$$

TABLE II. Theoretical parameter values used for calculating the thermal conductivity curves illustrated in Fig. 7 for different thermal conductivity behaviors.

	$2k_F/q_M$	γ	φ	Δ (K)
$PrAl_2$	4.15	0.125	0.014	44
$TbAl_2$	3.9	0.12	0.045	71
$TmAl_2$	4.15	0.00125	0.1	39

with

$$W=\begin{bmatrix} w_{11} & w_{12} \\ w_{21} & w_{22} \end{bmatrix}=\begin{bmatrix} \dfrac{A}{\sqrt{1+A^2}} & \dfrac{1}{\sqrt{1+A^2}} \\ \dfrac{1}{\sqrt{1+A^2}} & -\dfrac{A}{\sqrt{1+A^2}} \end{bmatrix}, \tag{A6}$$

where

$$A=\frac{h_z+\sqrt{\Delta^2+h_z^2}}{\Delta}. \tag{A7}$$

The self-consistent value for σ as defined above is given by

$$\sigma=\langle J^z\rangle=\frac{1}{Z}\sum_{\alpha}\langle\varepsilon_\alpha|J^z|\varepsilon_\alpha\rangle e^{-\beta\varepsilon_\alpha}, \tag{A8}$$

$$\beta=1/k_BT \quad \text{and} \quad Z=\sum_{\alpha} e^{-\beta\varepsilon_\alpha}.$$

k_B is the Boltzmann constant and T the temperature of the system. From the above equation we can easily obtain Eq. (2.3).

The matrix elements describing the magnetic scattering, the counterparts of the matrix elements $\mathcal{P}_{ij}^{(m)}$ in Sec. IV of Ref. 6, are

$$\begin{aligned}\frac{P_{ij}^s}{P_0^s}=&\frac{1}{4Z}\left[2(w_{12}^2w_{21}^2+w_{11}^2w_{22}^2)+(w_{22}w_{21}-w_{11}w_{12})^2\right]\\ &\times\left[e^{-\beta\varepsilon_1}R_{ij}(+h)+e^{-\beta\varepsilon_2}R_{ij}(-h)\right]+\frac{1}{Z}R_{ij}(0)\\ &\times\left[w_{21}^2w_{11}^2e^{-\beta\varepsilon_1}+w_{12}^2w_{22}^2e^{-\beta\varepsilon_2}\right]-\langle J^+\rangle\langle J^-\rangle R_{ij}(0)\\ &+\frac{1}{4Z}R_{ij}(0)\left[(w_{21}^2-w_{11}^2)^2e^{-\beta\varepsilon_1}\right.\\ &\left.+(w_{22}^2-w_{12}^2)^2e^{-\beta\varepsilon_2}\right]-\langle J^z\rangle^2R_{ij}(0).\end{aligned} \tag{A9}$$

P_0^s is a material constant.[6,7] The mean thermodynamical values are

$$\langle J^+\rangle=\langle J^-\rangle=\frac{1}{Z}\left[e^{-\beta\varepsilon_1}w_{11}w_{21}+e^{-\beta\varepsilon_2}w_{22}w_{11}\right] \tag{A10}$$

and $\langle J^z\rangle\equiv\sigma$ is determined self-consistently from Eq. (2.5) for the system in ferromagnetic phase and $\sigma=0$ in the paramagnetic phase.

The functions $R_{ij}(\eta h)$ read

$$\begin{aligned}R_{ij}(\eta h)=&\int_0^\infty d\varepsilon\int_0^\infty d\varepsilon'\left(-\frac{\partial f}{\partial\varepsilon}\right)F(\varepsilon,\varepsilon+\eta h)\\ &\times\delta(\varepsilon'-\varepsilon+\eta h)\,\nu_{ij}(\varepsilon,\eta h)\end{aligned} \tag{A11}$$

with $\eta=0,\pm1$ and where

$$\begin{aligned}\nu_{11}=&\varepsilon^{1/2}(\varepsilon+\eta h)^{1/2}(2\varepsilon+\eta h),\\ \nu_{12}=&\varepsilon^{1/2}(\varepsilon+\eta h)^{1/2}[(\varepsilon-\zeta)(2\varepsilon+\eta h)+\eta h(\varepsilon+\eta h)],\\ \nu_{22}=&\varepsilon^{1/2}(\varepsilon+\eta h)^{1/2}[(\varepsilon-\zeta)^2(2\varepsilon+\eta h)\\ &+2(\varepsilon-\zeta)\eta h(\varepsilon+\eta h)+(\eta h)^2(\varepsilon+\eta h)]\end{aligned} \tag{A12}$$

in which ζ is the chemical potential. For a degenerate electron gas we can put $\zeta=\varepsilon_F$, where ε_F is the Fermi energy counted from the bottom of a parabolic band structure modeling a complicated structure in general. The function $F(\varepsilon,\varepsilon')$ is defined as

$$F(\varepsilon,\varepsilon')=\frac{1}{1-f(\mathbf{k})\{1-\exp[\beta(\varepsilon,\varepsilon')]\}}, \tag{A13}$$

$$\beta=\frac{1}{k_BT}.$$

For the degenerate electron gas, after applying the standard Sommerfeld expansion, the functions (A11) can be represented by

$$R_{11}(x)=\frac{\zeta^2}{1+e^{-x}},$$

$$\begin{aligned}R_{12}(x)=R_{21}(x)=&\left[\frac{2x\zeta^2}{1+e^{-x}}-\frac{\pi^2}{3}(k_BT)\zeta^2\frac{1+e^{-x}}{(1+e^{-x})^2}\right.\\ &\left.+\frac{\pi^2}{3}(k_BT)^2\frac{8\zeta^2}{1+e^{-x}}\right],\end{aligned}$$

$$\begin{aligned}R_{22}(x)=&\left[\frac{2x^2}{1+e^{-x}}+\frac{\pi^2}{3}\frac{8(k_BT)^2x\zeta^2}{1+e^{-x}}\right.\\ &\left.-\frac{\pi^2}{3}(k_BT)x\zeta^2\frac{1-e^{-x}}{(1+e^{-x})^2}+\frac{\pi^2}{3}(k_BT)^2\frac{4\zeta^2}{1+e^{-x}}\right],\end{aligned} \tag{A14}$$

where $x=\eta h$ ($\eta=0,\pm1$). After inserting Eqs. (A2), (A6), and (A14) into Eq. (A9) we obtain Eqs. (3.5)–(3.8).

The application of Eq. (A14) in the cases of Ref. 6 leading to Eqs. (6-5) and (6-6) of that paper yield

$$\mathcal{P}_{11}^{(m)} = \Pi_J(T),$$

$$\mathcal{P}_{12}^{(m)} = \mathcal{P}_{21}^{(m)} = 2\left(\frac{\pi^2}{3}\right)\left(\frac{k_B T}{\varepsilon_F}\right)\Pi_J(T),$$

$$\mathcal{P}_{22}^{(m)} = \left(\frac{\pi^2}{3}\right)\Pi_J(T) - \Lambda_J(T) \tag{A15}$$

with

$$\Pi_J(T) = J(J+1) - \sigma^2 + \sigma \tanh\left(\frac{1}{2}x\right)$$

$$\Lambda_J(T) = \frac{(\pi^2/3)\sigma}{2[\cosh(x)+1]}x - \frac{1}{2}\frac{\sigma}{\sinh(x)}x^2, \tag{A16}$$

$$x = \frac{h_z}{k_B T}, \tag{A17}$$

and $\sigma = \langle J_z \rangle = Jm$. The above expression for $J = \frac{1}{2}$ corresponds to Eq. (3.6) in the case where $\Delta = 0$.

We should apologize for misprints in Ref. 6 where formulas (6-5) and (6-6) should be replaced by the correct formulas above. We expect that the use of the correct matrix elements above would not change the physical content of Ref. 6. Such corrected results applied to the thermoelectric power will be used in a following paper on that property.

*Electronic address: rassili@gw.unipc.ulg.ac.be
†Electronic address: durczew@int.pan.wroc.pl
‡Electronic address: ausloos@gw.unipc.ulg.ac.be

[1] I. A. Smirnov and V. S. Oskotski, in *Handbook on the Physics and Chemistry of Rare Earths*, edited by K. A. Gschneider and L. Eyring (North-Holland, Amsterdam, 1993), Vol. 16, p. 107.
[2] E. Gratz and M. J. Zuckermann, in *Handbook on the Physics and Chemistry of Rare Earths*, edited by K. A. Gschneider and L. Eyring (North-Holland, Amsterdam, 1982), Vol. 5, p. 117.
[3] F. J. Blatt, *Physics of Electronic Conduction in Solids* (McGraw-Hill, New York, 1968).
[4] P. G. Klemens, *Thermal Conductivity* (Academic, London, 1969).
[5] R. Berman, *Thermal Conduction in Solids* (Clarendon, Oxford, 1978).
[6] K. Durczewski and M. Ausloos, J. Magn. Magn. Mater. **51**, 230 (1985).
[7] A. Rassili and M. Ausloos, J. Magn. Magn. Mater. **147**, 341 (1995).
[8] A. Rassili and M. Ausloos, J. Magn. Magn. Mater. **163**, 153 (1996).
[9] A. Rassili and M. Ausloos, in *Magnetic Hysteresis in Novel Magnetic Materials*, Vol. 338 of Series E: Applied Sciences, edited by G. C. Hadjipanayis (Kluwer, Dordrecht, 1997), p. 187.
[10] K. Witanski, Phys. Status Solidi B **131**, 129 (1985).
[11] B. Bleaney, Proc. R. Soc. London, Ser. A **276**, 39 (1963).
[12] Y. L. Wang and B. Cooper, Phys. Rev. **172**, 539 (1968).
[13] P. Fulde and M. Loewenhaupt, Adv. Phys. **34**, 589 (1986).
[14] W. Bührer, M. Godet, H. G. Purwins, and E. Walker, Solid State Commun. **13**, 881 (1973).
[15] K. Kawasaki, Prog. Theor. Phys. **29**, 801 (1963).
[16] R. C. Mjolsness and W. M. Visscher, Phys. Fluids **15**, 1854 (1972).
[17] N. W. Ashcroft and N. D. Mermin, *Solid State Physics* (Holt-Saunders, London, 1976).
[18] T. Kasuya, Prog. Theor. Phys. **16**, 58 (1956).
[19] J. M. Ziman, *Electrons and Phonons* (Clarendon, Oxford, 1967).
[20] K. Durczewski and M. Ausloos, Phys. Rev. B **53**, 1762 (1996).